High efficient multifunctional self-heating nanocomposite based MWCNTs for energy applications

Mohammed Al-Bahrani [1,2]; Jasper Graham-Jones[1]; Vladimir Zholobenko[3]; Aqeel Al-Ani[2,3] ;Alistair Cree[1]

[1,3]Mechanical Engineering, School of Engineering, University of Plymouth, Plymouth, PL4 8AA, UK

[2] Iraqi Ministry of Oil, Baghdad, Iraq

[3]School of Chemical and Physical Sciences, Keele University, Keele, Staffordshire ST5 5BG, UK

Corresponding author: mohammed.naeem@plymouth.ac.uk

Abstract

Self-heating of conductive nanocomposite materials due to the joule heating effect is suitable for numerous engineering applications including self-healing, self-resin curing, de-icing, and adhesive bonded joints fabrication and so on. In this study a high efficiency self-heating nanocomposite based on high conductive multi-walled carbon nanotubes (MWCNTs) was fabricated using a hot-press method. The microstructure and the thermal stability of self-heating nanocomposite were studied by X-ray diffraction, scanning electronic microscopy and thermogravimetric tests. Electro-mechanical and electro-thermal performances tests were conducted to investigate their potential as a self-heating heater. Results showed that the compressive strength, Young's modulus and the piezoresistive behaviour were higher after adding MWCNTs to the phenolic resin, indicating better load transfer and self-damage sensing as well. Moreover, at 4.0 wt.% of MWCNTs concentration, the electrical conductivity of a self-heating nanocomposite showed a higher value and this result is strongly dependent on the sample thickness. In addition, a steady-state temperature of ≈ 110 °C could be reached at low applied volts (8V) as well as it's heating performance was significantly dependent on the input power and the thickness of the sample. Joule heating influence was also estimated analytically based on the one-dimensional heat transfer equation in companying with other previous model and the results reveal that the distributed temperatures values were very close to the experimental results. This type of self-heating nanocomposite has the potential to be used for various industrial applications sectors due to it's ability to self-damage sensing, easy fabrication, high heating efficient at low power consumption.

Keywords: Self-heating; joule effect; MWCNTs, Electro-mechanical properties.

1. Introduction

During the winter weather, the ice starts to form on surfaces of equipment and structures which causes a reduction in their performance. In addition, some materials for example in energy sectors (such as oil and its derivatives) are facing an increase in their viscosity due to the low-temperature conditions. This problem leads to a low flow rate of fluid inside the pipe line caused by high shear forces between the surface of the fluid and inside wall pipe surface. To address these issues, some conventional heating techniques have been utilized to minimize the effect of these issues. For example, infrared heating technique [1], induction heat [2], ultrasonic heating [3], hot air [4] and embedded heating element system [5] are often used. The main advantages of these conventional systems are they can heat a large area with a stable increase in temperatures. However, these systems need more tools to work and more time to heating large volumes in addition to costs. Electro-thermal materials such as copper, AL-alloys have been used for heating purpose due to their high thermal stability. However, the disadvantages of these materials are complicated manufacturing steps, heavyweight, and high power required to generate heat [6]. Therefore it is necessary to develop a new type of heater with higher heating efficiency to overcome these given issues.

Carbon nanotubes (CNTs) are considered one of the promising materials that can be used in different applications due to their superior mechanical, electrical and thermal properties [7-10]. CNT's improved mechanical properties additionally make polymers (i.e. nanocomposites) electrically conductive and work as a self-heating materials. Self-heating is defined as structure materials which can heat themselves by converting electrical energy to thermal energy. This occurs when electrical current passes through material exciting their electrons and atoms (i.e. Joule heating phenomenon).

Moreover, it has been proved that CNTs based nanocomposite as a self-heating heater has a rapid heating ability [11], and this property makes them an ideal candidate for heating applications in harsh conditions. Many studies have been carried out to use different types of nanocomposites based CNTs for self-heating applications. For instance, MWCNTs/epoxy [12, 13], CNTs/PDMS [14], MWCNTs/m-aramid [15], CNTs/polyurethane [16]. The above studies successfully incorporated CNTs within the polymer in order to fabricate a thin film used as a coating for a self-heating applications. However, it is impossible using this type of films to coating the inner pipe surface to heat and transport the oil (i.e. petrol) to mitigate it's viscosity. Additionally in some applications, there is a need to use a very strong polymer, unlike epoxy, as a matrix for self-heating nanocomposites, in order to endure high applied loads. Therefore, nano-coating and flexible materials (flexible self-heating materials) are not suitable to use in this case.

2. Experiments

In this study, we prepared self-heating nanocomposite containing different CNTs concentrations to develop a smart heating nanomaterial for different applications. Phenolic resin powder was chosen as a matrix for this type of self-heating nanocomposite heater due to its high mechanical and thermally stable properties. Electrical, mechanical and joule heating effect tests were investigated experimentally and theoretically in order to cover all possible occurred conditions. This type of self-heating heater can be used for winter conditions but also as a self-cleaning to remove waste oil (by melting) that accumulates on the surface of the structure.

2.1 Materials and sample

Multi-walled carbon nanotubes (MWCNTs) produced by chemical vapour depositing (CVD) were purchased from US-Research Nanomaterials Inc. (Houston, USA). The purity of MWCNTs is more than 97%, with a mean diameter of 40 nm and an average length of 35 μm. Therefore, the aspect ratio of MWCNTs has been found to be roughly 875. The phenolic resin which is in powder form, was purchased from (MetPrep Ltd, Coventry, UK) and used as a matrix material for sample preparation. All the materials in this study were used as received to prepare the self-heating nanocomposite samples without any further treatment.

2.2 Fabrication of CNTs/Phenolic nanocomposite

MWCNTs/Phenolic nanocomposites samples were fabricated using the hot pressing method using a mounting press machine (Bluhler2000, Leeds, UK). Different concentrations of MWCNTs ranging from (0 - 4 wt.%) were mixed with the phenolic powder and milled at 25 rpm for 2 h using a ball milling machine. The milling machine contains ceramic balls ranging from 25 to 60 mm in diameter. The mixture of MWCNTs/phenolic powders was cured at 150°C by a hot mounting press machine under a compression pressure of 10 MPa for 10 min and then 3 minutes as a cooling period see Figure 1.
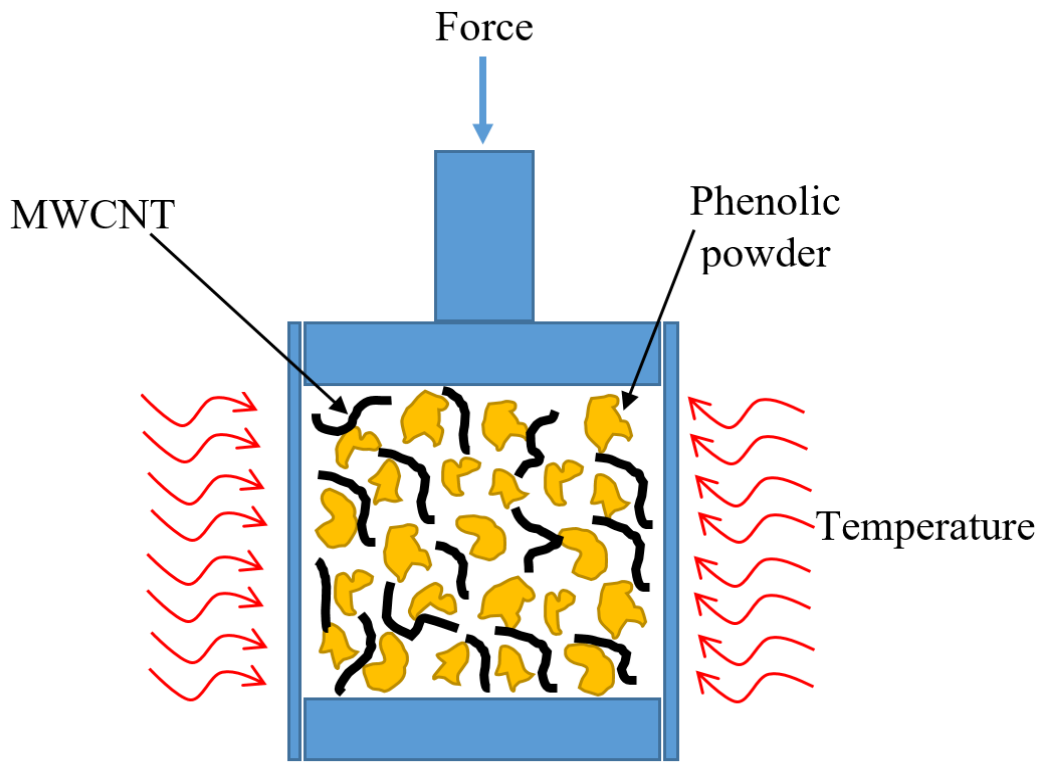
Figure 1. Scheck of the mounting hot press machine mould.

2.3 Characterizations

For the electrical measurements, a digital multimeter type (keithley 2100) was used to calculate the resistance of samples via a two-point probe method at room temperature. The specimen dimensions were 30×10×10 in mm and the volumetric electrical conductivity σ of the nanocomposite specimens was estimated by;

$$\sigma = \frac{L}{RA} \tag{1}$$

where *L*, *R* and *A* are the length, the resistance and the cross-section area of the nanocomposite sample, respectively. High purity silver paste was used on both ends of the specimens in order to ensure a good contact between the copper foil and nanocomposite specimen.

In order to investigate the electro-mechanical behaviour of the MWCNTs/phenolic nanocomposite, a compression test was carried out using a universal testing machine (Instron 5582, USA) with a 100 KN load cell and the test was performed at room temperature. A set of three cylindrical shape samples for each concentration with dimensions of length 25 mm and diameter 20 mm were tested with a constant crosshead speed of 1mm/min to obtain compression strength and compression modulus. The compression test procedures were carried out according to ASTM standard D695-08. For the cyclic test, three different strain amplitudes of 1%, 2% and 4% under three different loading

4

and unloading rates, (i.e. 0.4 mm/min, 0.8 mm/min and 1.2 mm/min) were conducted to investigate the effect of those test conditions on the nanocomposite piezoresistive properties. During the tests, the changes in electrical resistance (i.e. $\Delta R/R_0$ where ΔR is the change in the resistance of the specimen during the test and R_0 is the initial specimen's resistance) of the nanocomposite specimens were continuously recorded.

Scanning electronic microscopy (SEM) type (JEOL JSM-7001F, Japan) was used to exam the as-received MWCNTs and their degree of distribution inside the nanocomposite specimen's matrix. The fracture surface of the nanocomposite samples was coated first with a thin gold layer for bettering images before the examination.

Thermogravimetric analysis (TGA) was performed under nitrogen using a Rheometric Scientific STA-1500 instrument in order to calculate the weight loss of the nanocomposite samples. The samples were weighted carefully and heated from room temperature to 800 °C at a constant heating rate of 10 °C.min^{-1}.

A powder X-ray diffraction (XRD) test was employed to identify and characterise the morphological phase of the MWCNTs/phenolic nanocomposite containing different MWCNTs concentrations (i.e. 0 to 4wt. % of MWCNTs). BukerD8 X-Ray Diffractometer with Cu-Kα radiation generated under 40kv and 40 mA at room temperature was used to examine the specimens. The specimens are thoroughly ground to a fine powder and then placed in samples holder of the XRD-diffractometer. The XRD analysis was carried out at over the scanning angle 2θ and ranged between 5° and 28°.

To evaluate the joule heating performance of MWCNTs/phenolic nanocomposite, a joule heating principle was performed using a DC power source to generate heat inside the nanocomposite samples by controlling of the input voltage. The ends of samples were first attached with electrodes (i.e. copper tape) to allow the DC current to pass through the sample to generate heat. The temperature readings were obtained using a Wi-Fi thermocouple logger (EL-WiFi-TC, Dataq, Ohio, USA) and thermal images of the specimens during heating were captured using thermal infrared camera (TH7102MX, NEC, Japan) to show heat distribution in the samples. The power supply was calculated according to the power law;

$$P = I \times V \qquad (2)$$

Where, I is the current pass through the sample and V *is* the applied voltage.

3. Results and discussion

3.1 Electrical conductivity

Figure 2 shows the volume electrical conductivity of the MWCNTs nanocomposites as a function of MWCNTs loading. It can be seen that electrical conductivity of the nanocomposite is increased by about 10 orders of magnitude when the MWCNTs concentration is increased from (0 to 0.5%). This sharp increase in the nanocomposite conductivity is due to the formatting of the percolating network (percolation threshold) and a homogenous distribution of the MWCNTs within the nanocomposite, as shown in Figure 3b. Above the percolation threshold, when the MWCNTs concentration increases, the magnitude of the nanocomposite electrical conductivity gradually increased and showed a maximum value of 13.26 S/m at 4% wt. of MWCNTs concentration. The dispersion of MWCNTs in phenolic was further investigated by XRD test. Figure 4b shows the XRD patterns of both unmodified phenolic matrix and modified with different MWCNTs concentrations. All nanocomposites samples including the pure phenolic sample exhibit two diffraction peaks, a sharp one at $2\theta = 23°$ and the weaker one at $2\theta = 26.25°$. Moreover, increasing the content of MWCNTs in the nanocomposite samples, the diffraction peak intensities are found to be increased as well. The presence of these peaks with high intensities is due to the availability and uniform dispersion of MWCNTs within the phenolic matrix.
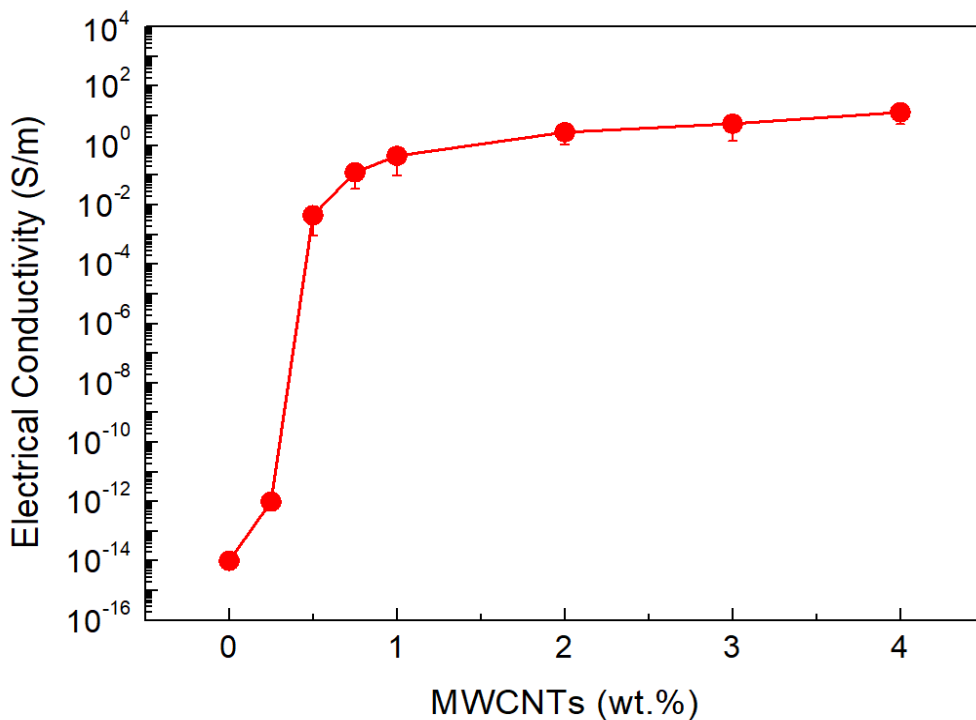
Figure 2. Electrical conductivity of MWCNTs/phenolic nanocomposite with different MWCNTs concentrations.

Furthermore, it was noted that although the percolated network of this type of the nanocomposite forms at MWCNTs loadings as low as 0.25 wt.%, the electrical conductivity of the MWCNTs/phenolic nanocomposite at this concentration is still very low in which to study the joule heating performance and obtain reliable results from the nanocomposite piezoresistive behaviour (i.e. electro-mechanical test). Moreover, to avoid the nanocomposite thermal degradation as well as a sudden increase in electrical resistance, samples which have a high electrical conductivity (i.e. at 4% wt. of MWCNTs) will maintain for all subsequent experiments. Table 1 summarises the statistical analysis results for samples above 0.5 wt.% of MWCNTs.

Table 1: Multiple comparison summery between the samples with different MWCNTs concentrations

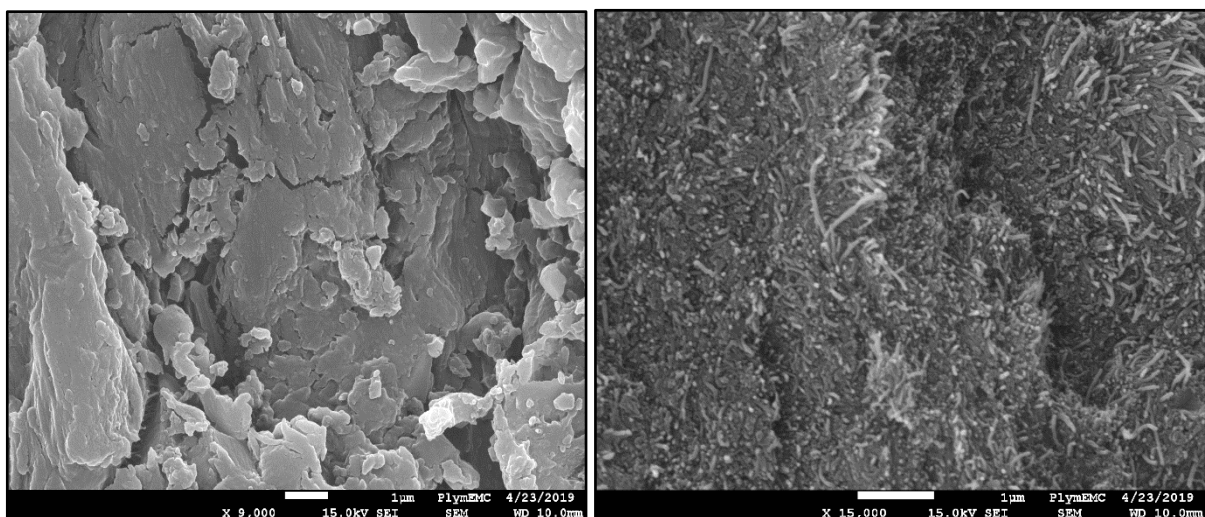| Tukey's Multiple comparison tests	P-value	Summery
1 wt. % MWCNTs VS. 2.0 wt.% MWCNTs	0.04	significant difference
2 wt. % MWCNTs VS. 3.0 wt.% MWCNTs	0.07	No significant difference
2 wt. % MWCNTs VS. 4.0 wt.% MWCNTs	0.06	No significant difference

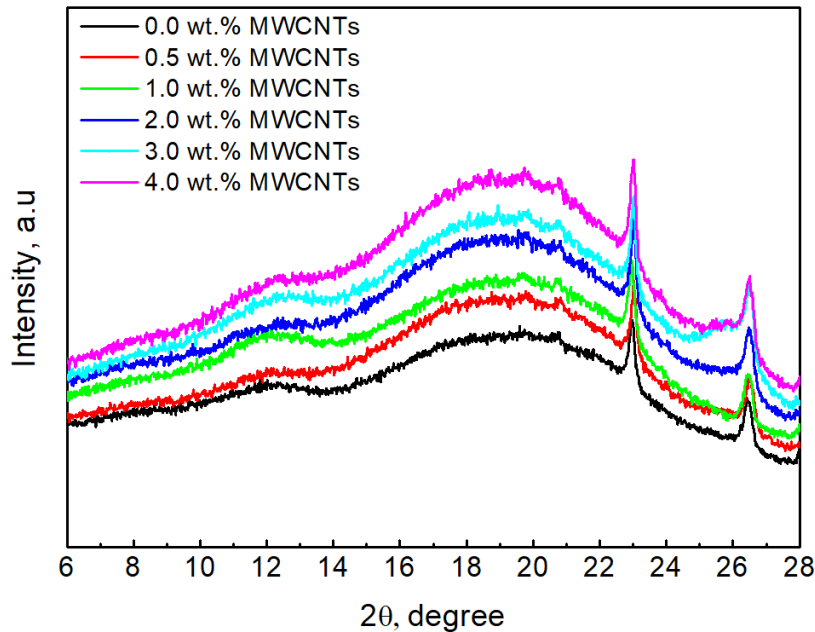**Figure 3**. SEM images (a) pure phenolic resin (b) 4 wt. % MWCNTs/phenolic nanocomposite.

Figure 4. X-ray diffraction pattern for pure phenolic resin and MWCNTs/phenolic nanocomposites containing different MWCNTs concentrations.

3.2 Electro-Mechanical properties of the nanocomposite

The results of the typical static compression mechanical stress-strain and the piezoresistive measurements ($\Delta R/R_0$) for the static loading until sample fracture are shown in Figure 5 and Figure 6, respectively. From Figure 5, it can be seen that the mechanical properties for the nanocomposite samples containing 4 wt. % of MWCNTs were observed to be remarkably increased as compared with unmodified phenolic samples. For instance, the specific compression strength and specific compression modulus (see Figure 5 inset) were improved by $\approx$ 11.1 % and $\approx$ 28.7% respectively, compared to unmodified phenolic samples. This improvement in mechanical properties is attributed to a high aspect ratio and a uniform dispersion of the MWCNTs in the phenolic matrix, as shown in Figure 3a, b. In addition, a strong interfacial bond between the MWCNTs and the phenolic matrix, which is confirmed by XRD test as Figure 4, helps the load to transfer in straightforward between the nanocomposites components [17, 18].
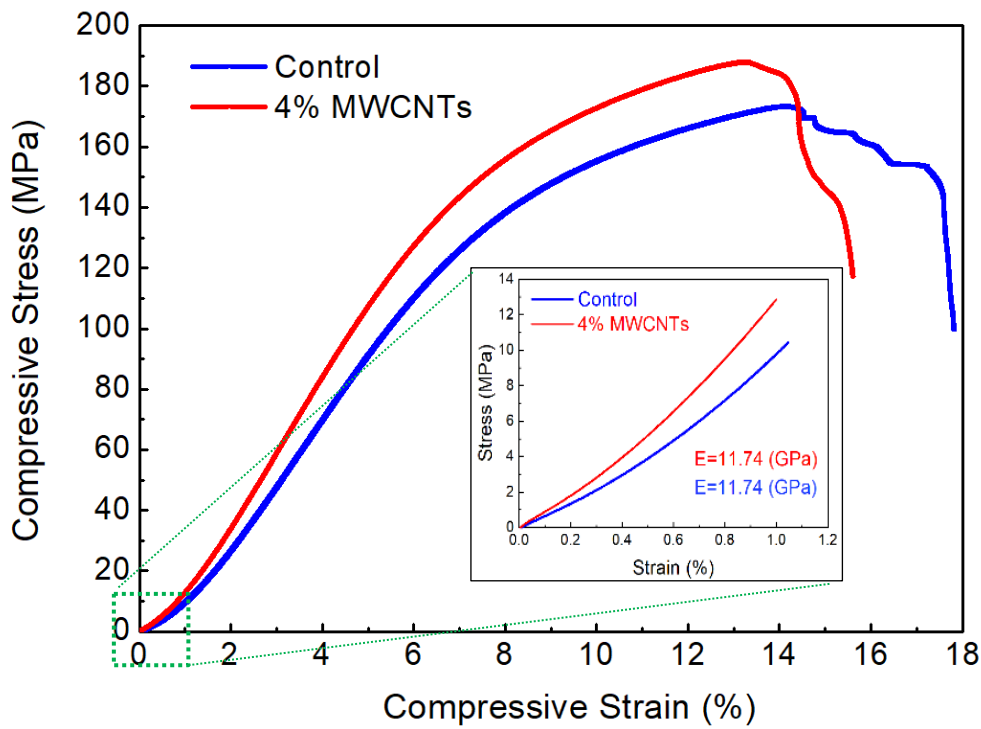
Figure 5. Relationship of compressive stress vs. strain for pure phenolic resin and 4 wt.% MWCNTs/phenolic nanocomposite.

Regarding the piezoresistive behaviour of the MWCNTs/phenolic nanocomposite, Figure 6 shows the variation of the compression stress and the relative changes in resistance as a function of compression strain. It can be observed that the values of the relative change in resistance ($\Delta R/R_0$) decreased linearly as the applied strain increased up to 13 % of strain, which is defined as the negative strain effect [19], and then increased. This is attributed to a reduction in the distance between CNT-CNT, which is known as a tunnelling distance according to Simons' theory [20]. A reduction in these gaps leads to decrease in the specimen electrical resistance [21]. After which (i.e. when the strain exceeds 13%), the relative change in resistance started to increase. This is due to the cracks in the matrix being initiated and spread within the nanocomposite matrix in different directions. These cracks cause an increase in the gaps between MWCNTs as well as distorting MWCNTs network paths which prevents electrons from passing easily through them and as a consequence the overall electrical resistance of the specimen increases [22]. This test is important to be considered for design as well as in order to obtain a better observation for the behaviour of a structure made from this type of the self-heating nanocomposite when it is being exposed to a load.

9
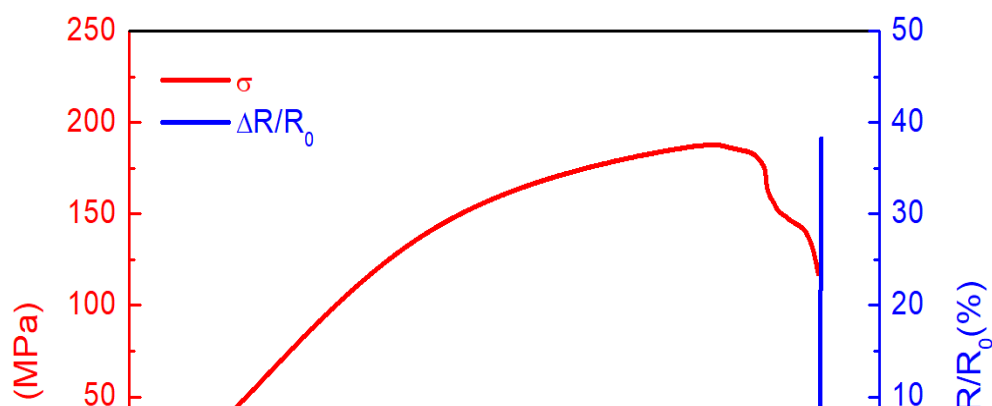
3.3 The effect of sample thickness on electrical resistance

Different sample thicknesses of 4.0 wt.% of MWCNTs/phenolic nanocomposite were prepared to investigate the effect of thickness changes on their electrical properties. Figure 7 shows the variations in electrical conductivity and resistance for MWCNTs/phenolic nanocomposite samples as a function of thicknesses. It can be noted that the electrical conductivity of the samples (which is calculated from Eq. 1) significantly increased when the thickness of the MWCNTs/phenolic nanocomposite samples increased as well. In contrast, it was also observed that the electrical resistance of the nanocomposite samples dropped remarkably as the samples thickness increased. For example, the sample that has a thickness of 10 mm showed the lowest value in terms of electrical resistance which was 12.8Ω and this value is $\approx$ 49% lower than that of a 3.0mm thickness. That is also confirmed by statistical calculation between the samples in terms of their electrical properties, for example, (P-value <0.0001) showed a high significant difference between 3.0mm and 10.0mm thickness. This reduction in sample resistance is due to an increase occurred in the density of MWCNTs networks. The increase in CNT-CNTs contacts helps to minimise the tunnelling resistance between them and allows more numbers of electrons to be easily transferred through the nanocomposite sample.
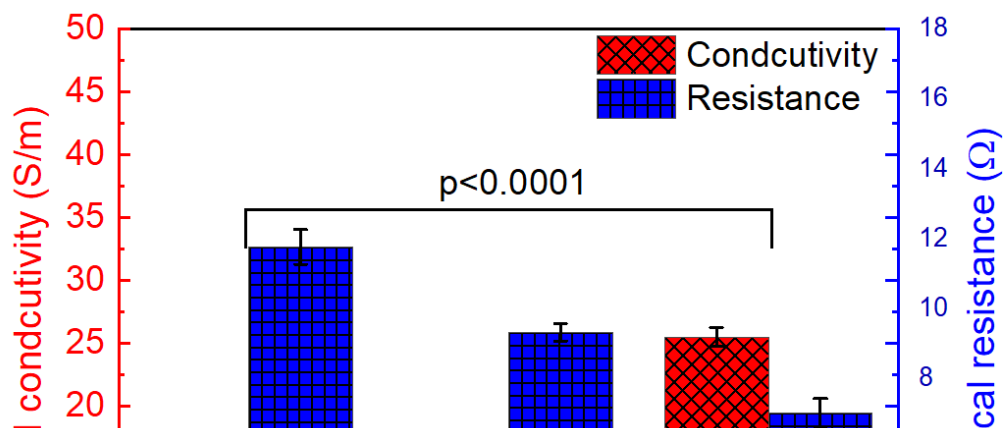
3.4 The temperature profile of MWCNTs/phenolic nanocomposite

The major purpose of this study is to investigate the possibility of this type of MWCNTs/phenolic nanocomposite to be used as a self-heating heater. Therefore, considering that the application of the studied nanocomposite material could be used at a relatively high working temperature in this study, samples with an area of 30×26 mm^2 with different thicknesses were prepared and tested under different applied voltages for a certain time. Figure 8a, and b show the temperature plots for two thicknesses of MWCNTs/phenolic nanocomposite samples (i.e. 3 mm and 10 mm). It can be noted that the steady state of temperature was observed to increase in a linear pattern with an increased in the applied voltages. This is due to the joule heating influences and based on the power law as Eq. 2; the applied electrical current is fully converted to heat [23]. The increase in temperatures was also noted to be fast; for instance, the less thick sample offered maximum temperatures of 28 and 49 °C which were induced at applied voltages of 8 and 10V, respectively. In addition to that, if the applied voltage increases to 12V, that led to an increase in the sample's temperature to 70C. However, the sample with the 10mm thickness (see Figure 8b) showed a higher temperature at relatively lower applied voltages. For example, a maximum saturation temperature at 8 V was ≈ 109 °C, which is much higher (compared to the same applied voltage) with that sample has a 3mm thickness. This is because of the lower electrical resistance of the thick MWCNTs/phenolic sample, as confirmed in Figure 7. In addition, it can be inferred from the results that the samples with lower electrical

resistance showed the higher state of temperatures with rapidly increasing rate with uniform temperature distribution (as shown in Figure 8) as compared to previous systems [24].
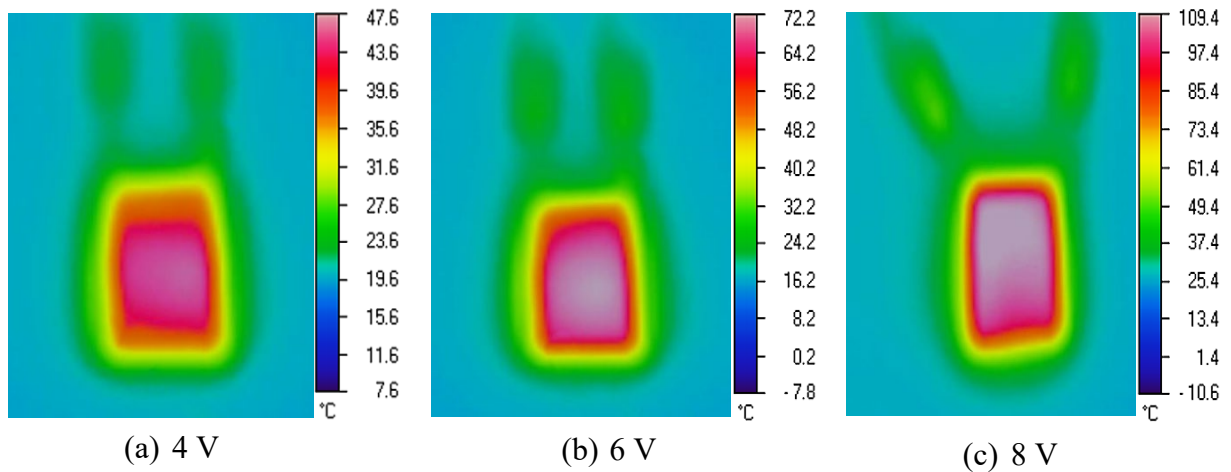

(a) 4 V   (b) 6 V   (c) 8 V

Figure 9. Infrared thermal images of the MWCNTs/phenolic nanocomposite heater (10 mm thick) for different applied voltages: (a) 4V; (b) 6 and (c) 8 V.

3.5 Electro-thermal response of MWCNTs/phenolic nanocomposite

The influence of temperature of the electrical resistance changes of MWCNTs/phenolic nanocomposite is shown in Figure 9 using a 10mm thick sample after exposure to high temperatures (see Figure 8b).
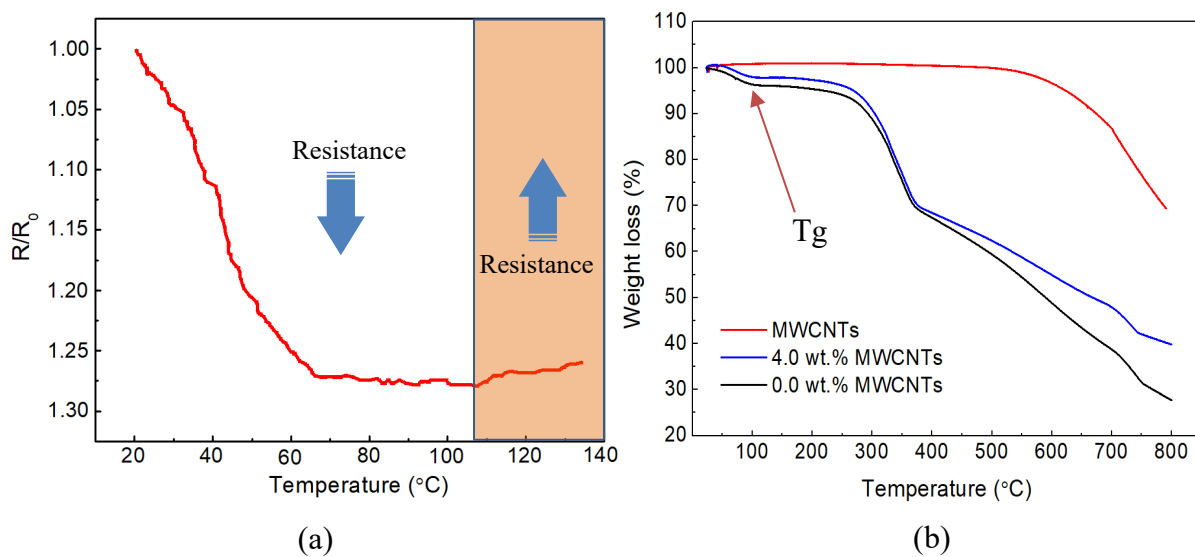

(a)   (b)

Figure 10. (a) Normalized change in resistance as a function of temperature for 10 mm thickness of 4wt.% MWCNT/phenolic nanocomposite and (b) thermogravimetric analysis (TGA) vs. temperature.

12

It can be observed that the normalised resistance decreases in a nonlinear behaviour when the temperature increased from 20 C to 110 C. Thus this type of nanocomposite showed a negative temperature coefficient (NTC) trend. This behaviour can be elaborated on as the temperature increases, the gaps between MWCNT to MWCNT will reduce because the thermal expansion of the matrix (i.e. phenolic resin) decreased. This reduction in matrix thermal expansion is due to the shrinking of phenolic resin chains, and as a result, new conductive paths (i.e. increasing the number of contacts between MWCNTs) have been generated [14, 25]. NTC also appeared in different type nanocomposites based CNTs in many previous studies [25, 26] and it also can be affected by different factors such as the type of polymer, aspect ratio and concentration of CNTs [14]. However, when the temperature exceeded ≈ 110 C a positive temperature coefficient (PTC) trend appeared and showed an increase in normalised resistance. This is due to the degradation in the matrix chains (i.e. glass transition temperature Tg) and caused the break of MWCNTs conductive paths as well as increasing the inter-tubes (MWCNTs) gaps as a consequence, and based on the tunnelling resistance theory, the sample resistance will increase [27]. This sudden change in the matrix (i.e. Tg) is also confirmed by the thermogravimetric analysis (TGA) test (Figure 9b). In general, the NTC trend of the MWCNTs/phenolic nanocomposite is important for the self-heating nanocomposite applications through exploiting this phenomenon to reduce the power consuming based on Eq.2.

3.6 The efficiency of this type of self-heating nanocomposite heater

The heat generated inside the MWCNTs/phenolic nanocomposite specimen is a result of the Joule heating effect. In this study, Joule heating occurs when electric current passes through nanocomposite materials and it's inherent resistance leads to convert the electrical energy to thermal. Therefore, the power consumption of the self-heating MWCNTs/phenolic nanocomposite to generate heat can be calculated from Eq.(3) which is equal to;

$$p = \frac{\psi}{t} = I^2 \times R = V^2 \times R \tag{3}$$

Where p is the power consumption, and Ψ is the heat generated, and t is the time required to generate this heat. Figure 10 shows the power consumption as a function of voltages applied for two thicknesses of MWCNT/phenolic nanocomposite specimens. It can be noted that the sample with

high thickness needs less power to generate heat compared with the thin sample at the same applied voltage. This is due to the excellent electrical conductivity of thick MWCNTs/phenolic samples (i.e. less resistance) obtained from high contact between MWCNTs. From the graph in Figure 10, there is clearly a statically significant difference between the sample with thick-10 mm and thick-mm in terms of power consumption in which (p-value ≈ 0.0001). Form this, it can be inferred that the self-heating nanocomposite heater with less thickness would not to be the best option, and a thick sample would be preferred.
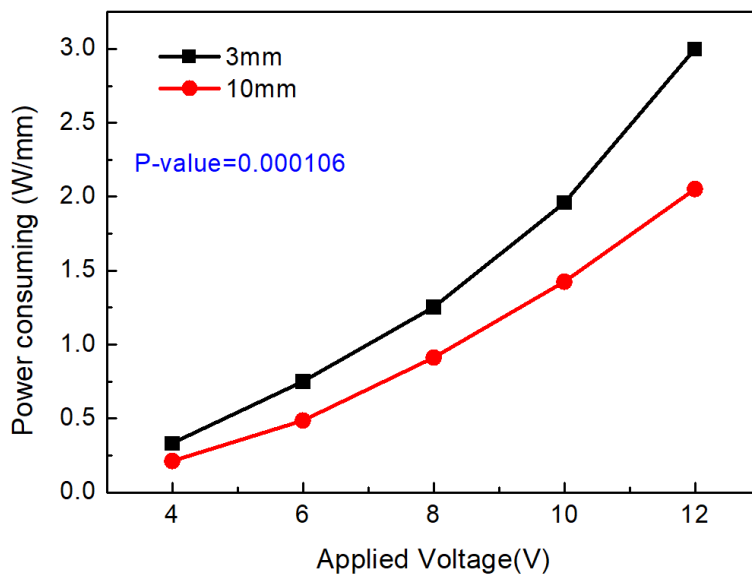
Figure 11. Power consuming verses applied voltages for different thickness of 4 wt.% MWCNTs/phenolic nanocomposite.

3.7 Estimation of temperature distribution

To estimate the temperature distribution of MWCNTs/phenolic nanocomposite with applied voltage, a steady-state one-dimensional heat transfer equation [28] was dependent in this study as the model. The Heat generated (Ψ) by the current in the MWCNTs/phenolic specimen is assumed as;

$$\Psi = d \times h = \frac{V^2}{A^2 \times R^2 \times \sigma} \tag{4}$$

Where, d is current density which is equal to electrical current (I) divided by the sample's effective cross-section area (A), and h is the electrical field which is equal to the applied voltage divided by distance between two electrodes (i.e. sample length L), and σ is the sample's electrical conductivity. The Joule heating effect is illustrated in Figure 11.
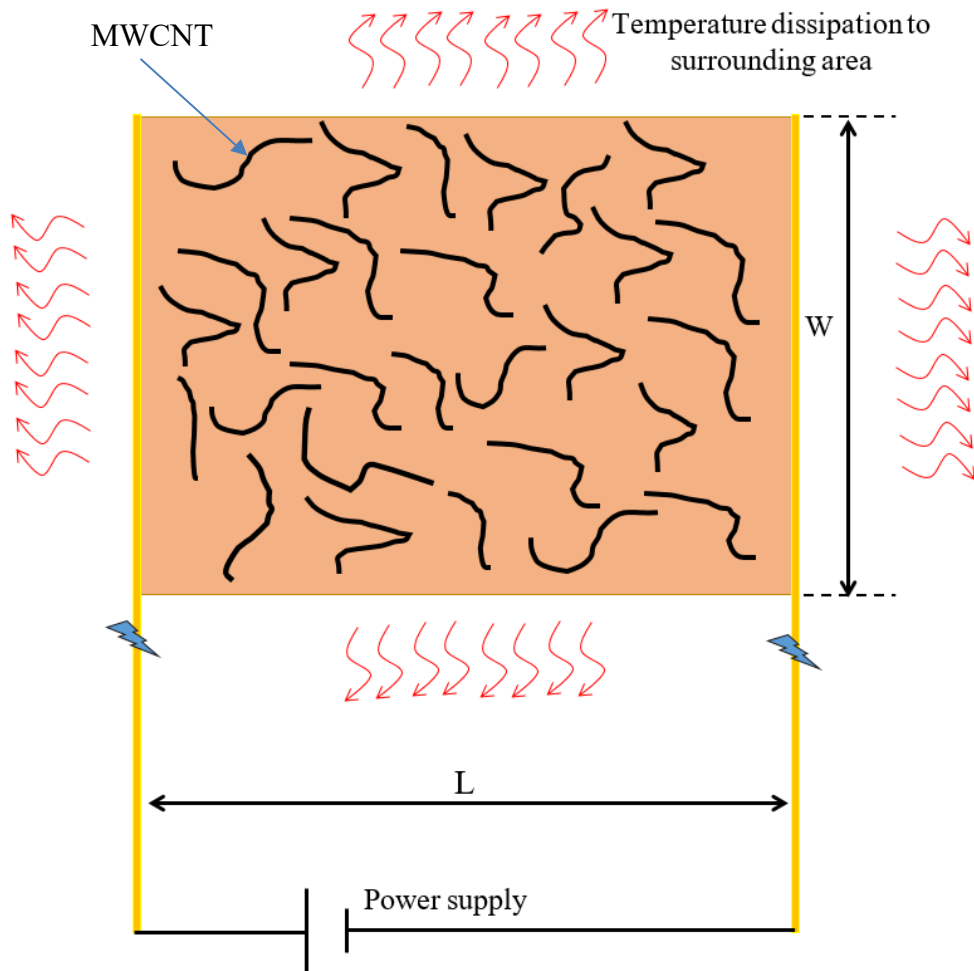

Figure 12. Schematic plot of the joule heating effect on the self-heater nanocomposite.

In this study, we can assume that the temperature distribution through the specimen is T(x) is defined as the difference between the ambient temperature θ_0 (surrounding temperature) and the local temperature $\theta(x)$. Therefore, the heat equation can be given by;

$$\frac{d^2T}{dx^2} - \frac{\beta}{k} \times \frac{dT}{dx} + \frac{\Psi}{k} = 0 \qquad (5)$$

Where k is the thermal conductivity of self-heating MWCNTs/phenolic nanocomposite. β is the coupling coefficient and assumed as h/w to remain constant along with the specimen [29], where h indicates the air heat convection coefficient, and w is the effective nanocomposite width. For this model, the air convection coefficient can be assumed (100 W/m^2.k). Integration process has been conducted to solve Eq.(5) based to the following boundary conditions which were assumed (x = 0 at the mid of the specimen and at x = $\pm$ L/2 (i.e. at both specimens ends, dT = 0). Therefore, the temperature distributed along with the specimen, after applied the given boundary conditions and by combining with Eq.(4), the final relationship can be given as;

$$T(x) = \frac{V^2}{kA^2R^2\alpha^2\sigma}\left[1 - \frac{\cosh(\alpha x)}{\cosh(\frac{\alpha L}{2})}\right] \qquad (6)$$

Where, $\alpha = \sqrt{\beta/k}$. Self-heating MWCNT/phenolic nanocomposite thermal conductivity (k) and electrical conductivity (σ) are also needed to utilize Eq.(6). Therefore, the electrical conductivity, can be obtained from Figure 2, and regarding the thermal conductivity, in this study we assume that it can be calculated from the following relations [30],

$$k = k_m + \frac{\delta^2\phi k_m k_c}{3(k_m + \delta k_c H(\delta\eta)} \qquad (7)$$

Where k is the effective thermal conductivity of the MWCNTs/phenolic nanocomposite, k_c and ϕ indicate the thermal conductivity and the volume fraction of the MWCNT. It is well known that the thermal conductivity of the MWCNT (K_c) is high and ranges from 600 – 6000 W.m^{-1}.k^{-1} [8].

16

Therefore, in our simulations, we use 3000 W.m^{-1}.K^{-1} in accordance with some previous studies as well as the (K_m) is about 0.2 W.m^{-1}.K^{-1} for most polymers [31]. The parameter, δ, indicates the non-straightness of the MWCNT; this parameter can only be considered here if the aspect ratio (l/d) of the MWCNT is high. However, based on the current specifications of the MWCNTs in this study (i.e. the aspect ratio (η) is approximately 875 and this value is considered low, based on some recent studies [32]. Therefore, the non-straightness parameter (δ) is considering unity in this study. Moreover, H is defined as a depolarisation factor, this factor reflects the influence of the MWCNT aspect ratio (η) on the thermal conductivity of nanocomposite and can be given as [33]:

$$H(\eta) = [(\eta\sqrt{(\eta^2-1)}) \times \ln[\eta + \sqrt{(\eta^2-1)}] - 1] / (\eta^2 - 1) \tag{8}$$

Figure 13 shows the temperature profile of a 30 mm long self-heating MWCNTs/phenolic nanocomposite containing 4% wt. of MWCNTs. It can be noted that the temperature increases with a higher applied voltage and was at the middle of the specimen higher than both ends of specimen, this is due to the heat at the ends which is dissipated quickly to the surrounding area by convection. In addition, when the applied voltage is 4 volts, this showed a predicted temperature (36.2 °C) and about (97.1°C) when the applied volt increases to 8 volts. Therefore, it can be inferred that the results obtained from the one-dimensional stead-state heat transfer equation combined with effective nanocomposite thermal conductivity equations give very close values to the experimental work. Furthermore, this quantitative criterion is considering a good model to estimate Joule heating influence on increasing of self-heating MWCNTs/phenolic nanocomposite temperatures.
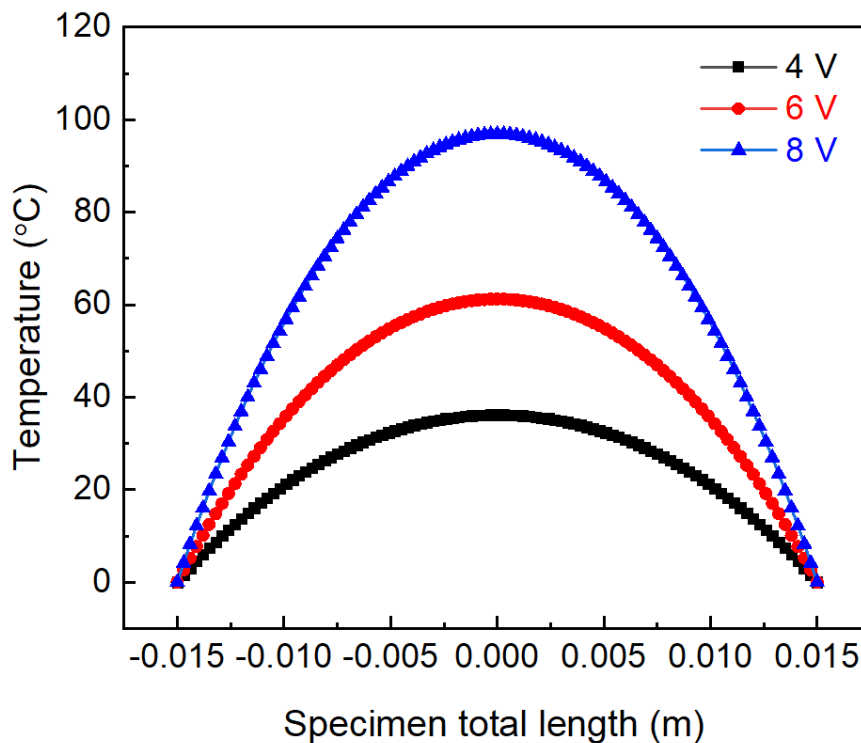
Figure 13. Simulated temperature profile along length of a 10mm thick of self-heating MWCNTs/phenolic nanocomposite specimen containing 4 wt. % MWCNTs at various applied voltages.

4. Conclusions

In summary, a self-heating nanocomposite was fabricated as a simple method for heating applications. The electro-mechanical and electro-thermal properties of these self-heating nanocomposites were systemically studied. Due to the uniform dispersion of MWCNTs in the phenolic matrix, an enhancement in the electrical conductivity was achieved and found to increase by several orders after incorporating MWCNTs, and the high value was at 4.0 % of MWCNTs concentration. A significant improvement in mechanical properties was also obtained, the compression strength and Young's modulus were enhanced by ≈ 11.1 % and $\approx 28.7\%$ respectively, by the adding of 4.0 wt. % of MWCNTs, compared to unmodified phenolic samples. Self-heating nanocomposite exhibits a good piezoresistive behaviour when subjected to compression load, revealing that it can able to sense any damage occurred during the service. Joule heating effect was also carried out to investigate the performance of self-heating the MWCNTs/phenolic nanocomposite. The temperature profile of the MWCNTs/phenolic samples was uniformly distributed and strongly affected by the sample's thickness at the same voltage applied. The MWCNT/phenolic nanocomposite thickness of the sample was also dominated in terms of power consumed, in statistical analysis point of view; a 10mm sample thick shows a significant difference in lower power consuming (i.e. p-value ≈ 0.0001) compared with 3mm sample thickness. Moreover, Joule heating influence was modelled in terms of temperature distributed and results from a predictive temperature distribute profile were very close to those experimentally obtained. Therefore, the obtained results clearly exhibit the efficiency of this type of self-heating nanocomposite and could be considered as a promising candidate in terms of low cost, high efficient heating, and self-damage sensing for varies type of applications.

References

[1] Vollmer M, Möllmann K-P. Infrared thermal imaging: fundamentals, research and applications: John Wiley & Sons; 2017.

[2] Rudnev V, Loveless D, Cook RL. Handbook of induction heating: CRC press; 2017.

[3] Yaralioglu G. Ultrasonic heating and temperature measurement in microfluidic channels. Sensors and Actuators A: Physical. 2011;170:1-7.

[4] Parent O, Ilinca A. Anti-icing and de-icing techniques for wind turbines: Critical review. Cold regions science and technology. 2011;65:88-96.

[5] Alam MNHZ, Schäpper D, Gernaey KV. Embedded resistance wire as a heating element for temperature control in microbioreactors. Journal of Micromechanics and Microengineering. 2010;20:055014.

[6] Janas D, Koziol K. A review of production methods of carbon nanotube and graphene thin films for electrothermal applications. Nanoscale. 2014;6:3037-45.

[7] De Volder MF, Tawfick SH, Baughman RH, Hart AJ. Carbon nanotubes: present and future commercial applications. science. 2013;339:535-9.

[8] Lekawa-Raus A, Patmore J, Kurzepa L, Bulmer J, Koziol K. Electrical properties of carbon nanotube based fibers and their future use in electrical wiring. Advanced Functional Materials. 2014;24:3661-82.

[9] Jyoti J, Basu S, Singh BP, Dhakate S. Superior mechanical and electrical properties of multiwall carbon nanotube reinforced acrylonitrile butadiene styrene high performance composites. Composites Part B: Engineering. 2015;83:58-65.

[10] Al-Bahrani M, Aljuboury M, Cree A. Damage sensing and mechanical properties of laminate composite based MWCNTs under anticlastic test. Materials Research Express. 2018;6:035704.

[11] Janas D, Koziol KK. Rapid electrothermal response of high-temperature carbon nanotube film heaters. Carbon. 2013;59:457-63.

[12] Neitzert HC, Vertuccio L, Sorrentino A. Epoxy/MWCNT composite as temperature sensor and electrical heating element. IEEE Transactions on Nanotechnology. 2011;10:688-93.

[13] Wang F, Liang W, Wang Z, Yang B, He L, Zhang K. Preparation and property investigation of multi-walled carbon nanotube (MWCNT)/epoxy composite films as high-performance electric heating (resistive heating) element. Express Polymer Letters. 2018;12.

[14] Chu K, Park S-H. Electrical heating behavior of flexible carbon nanotube composites with different aspect ratios. Journal of industrial and engineering chemistry. 2016;35:195-8.

[15] Jeong YG, Jeon GW. Microstructure and performance of multiwalled carbon nanotube/m-aramid composite films as electric heating elements. ACS applied materials & interfaces. 2013;5:6527-34.

[16] Luo J, Lu H, Zhang Q, Yao Y, Chen M, Li Q. Flexible carbon nanotube/polyurethane electrothermal films. Carbon. 2016;110:343-9.

[17] Bhattacharya M. Polymer nanocomposites—a comparison between carbon nanotubes, graphene, and clay as nanofillers. Materials. 2016;9:262.

[18] Liu W, Wei B, Xu F. Investigation on the mechanical and electrical properties of carbon nanotube/epoxy composites produced by resin transfer molding. Journal of Composite Materials. 2017;51:2035-43.

[19] Bilotti E, Zhang R, Deng H, Baxendale M, Peijs T. Fabrication and property prediction of conductive and strain sensing TPU/CNT nanocomposite fibres. Journal of Materials Chemistry. 2010;20:9449-55.

[20] Yu Y, Song G, Sun L. Determinant role of tunneling resistance in electrical conductivity of polymer composites reinforced by well dispersed carbon nanotubes. Journal of Applied Physics. 2010;108:084319.

[21] Bao W, Meguid S, Zhu Z, Weng G. Tunneling resistance and its effect on the electrical conductivity of carbon nanotube nanocomposites. Journal of Applied Physics. 2012;111:093726.

[22] Arjmand M, Mahmoodi M, Gelves GA, Park S, Sundararaj U. Electrical and electromagnetic interference shielding properties of flow-induced oriented carbon nanotubes in polycarbonate. Carbon. 2011;49:3430-40.

[23] Chu K, Yun D-J, Kim D, Park H, Park S-H. Study of electric heating effects on carbon nanotube polymer composites. Organic Electronics. 2014;15:2734-41.

[24] Rezaie B, Rosen MA. District heating and cooling: Review of technology and potential enhancements. Applied energy. 2012;93:2-10.

[25] Chu K, Kim D, Sohn Y, Lee S, Moon C, Park S. Electrical and thermal properties of carbon-nanotube composite for flexible electric heating-unit applications. IEEE Electron Device Letters. 2013;34:668-70.

[26] Mohiuddin M, Hoa S. Temperature dependent electrical conductivity of CNT–PEEK composites. Composites Science and Technology. 2011;72:21-7.

[27] Chu K, Lee S-C, Lee S, Kim D, Moon C, Park S-H. Smart conducting polymer composites having zero temperature coefficient of resistance. Nanoscale. 2015;7:471-8.

[28] Bergman TL, Incropera FP, Lavine AS, DeWitt DP. Introduction to heat transfer: John Wiley & Sons; 2011.

[29] Kitsuki H, Yamada T, Fabris D, Jameson JR, Wilhite P, Suzuki M, et al. Length dependence of current-induced breakdown in carbon nanofiber interconnects. Applied Physics Letters. 2008;92:173110.

[30] Deng F, Zheng Q. Interaction models for effective thermal and electric conductivities of carbon nanotube composites. Acta Mechanica Solida Sinica. 2009;22:1-17.

[31] Chen H, Ginzburg VV, Yang J, Yang Y, Liu W, Huang Y, et al. Thermal conductivity of polymer-based composites: Fundamentals and applications. Progress in polymer science. 2016;59:41-85.

[32] Kumar RM, Sharma SK, Kumar BM, Lahiri D. Effects of carbon nanotube aspect ratio on strengthening and tribological behavior of ultra high molecular weight polyethylene composite. Composites Part A: Applied Science and Manufacturing. 2015;76:62-72.

[33] Deng F, Zheng Q-S, Wang L-F, Nan C-W. Effects of anisotropy, aspect ratio, and nonstraightness of carbon nanotubes on thermal conductivity of carbon nanotube composites. Applied Physics Letters. 2007;90:021914.